



Cite this: *Biomater. Sci.*, 2023, **11**, 6537

A precise design strategy for a cell-derived extracellular matrix based on CRISPR/Cas9 for regulating neural stem cell function†

Yuanxin Zhai,^a Lingyan Yang,^a  *^a Wenlong Zheng,^b Quanwei Wang,^a Zhanchi Zhu,^a Fang Han,^a Ying Hao,^a Sancheng Ma^{*b} and Guosheng Cheng^{*a,c}

The extracellular matrix (ECM) is a natural microenvironment pivotal for stem cell survival, as well as proliferation, differentiation and metastasis, composed of a variety of biological molecular complexes secreted by resident cells in tissues and organs. Heparan sulfate proteoglycan (HSPG) is a type of ECM protein that contains one or more covalently attached heparan sulfate chains. Heparan sulphate chains have high affinity with growth factors, chemokines and morphogens, acting as cytokine-binding domains of great importance in development and normal physiology. Herein, we constructed endogenous HSPG2 overexpression in mouse embryonic fibroblasts based on the CRISPR/Cas9 synergistic activation mediator system and then fabricated a cell-derived HSPG2 functional ECM (ECM^{HSPG2}). The ECM^{HSPG2} is capable of enriching basic fibroblast growth factor (bFGF), which binds more strongly than the negative control ECM. With a growing bFGF concentration, ECM^{HSPG2} could better maintain neural stem cell (NSCs) stemness and promote NSC proliferation and differentiation in culture. These findings provide a precise design strategy for producing a specific cell-derived ECM for biomaterials in research and regenerative medicine.

Received 9th September 2022.

Accepted 13th March 2023

DOI: 10.1039/d2bm01466a

rsc.li/biomaterials-science

Introduction

Stem cell survival, maintenance, proliferation, differentiation and metastasis are regulated by the microenvironment that they reside in.^{1–3} The microenvironment regulates stem cell fate through specific niche components, including supporting cells, growth factors and the extracellular matrix (ECM).^{4,5} The ECM is the natural microenvironment for all cells in the body, produced and secreted by resident cells in tissues or organs.⁶ The complicated relationship between stem cells and their surrounding ECM is a crucial control mechanism for stem cell function. The ECM derived from human umbilical vein endothelial cells could promote osteogenic differentiation of human bone marrow mesenchymal stem cells.⁷ It has been shown that the ECM is a vital regulator of epidermal stem cell fate, and destructive ECM components could impair epidermal

stem cell homeostasis and morphogenesis.⁸ A cell-derived ECM with suitable hydrophilic properties could promote neural progenitor cell adhesion, proliferation and differentiation into basal forebrain cholinergic neurons.⁹ The ECM could be a favourable cell culture carrier for neural progenitor cell attachment and has great application potential in cell therapy for Alzheimer's disease.

Although these basic functions are well defined, currently little is known about ECM individual components and their roles in stem cell fate regulation. One of the major challenges in the fields of tissue engineering and regenerative medicine is unravelling this mystery and designing biomaterials to repair or replace damaged tissues and organs. Nowadays, most ECM proteins have been well described and characterized. Complex ECM proteins can be classified into two main types: structural matrix proteins and proteoglycans.¹⁰ Collagens, laminin, fibronectin and elastin are major structural proteins that provide the structural support and biomechanical stability for tissues.¹¹ Proteoglycans, which consist of a core protein and one or more covalently bound glycosaminoglycan chains, play many essential roles in biological processes, including development and disease progression.^{12,13} Heparan sulfate proteoglycan (HSPG) is one kind of proteoglycan consisting of a core protein with several covalently attached heparan sulfate chains, and it is widely distributed on the cell surface and in the ECM, where it interacts with a variety of ligands to regulate cellular function.¹⁴ Over the last decade, the binding pro-

^aCAS Key Laboratory of Nano-Bio Interface, Suzhou Institute of Nano-Tech and Nano-Bionics, Chinese Academy of Sciences, Suzhou, Jiangsu 215123, China.

E-mail: lyy2013@sinano.ac.cn, gscheng2006@sinano.ac.cn

^bSuzhou Kowloon Hospital, Shanghai Jiaotong University Medical School, Suzhou, Jiangsu 215123, China. E-mail: sanchengma@hotmail.com

^cGuangdong Institute of Semiconductor Micro-Nano Manufacturing Technology, Guangdong 528200, China

† Electronic supplementary information (ESI) available: The detailed information for essential reagents, sequences of the sgRNA and real-time PCR primers, mRNA expression and protein expression of HSPG2 in three sgRNAs transfected MEFs. See DOI: <https://doi.org/10.1039/d2bm01466a>



properties of these chains have attracted more attention. Heparan sulfate chains have high affinity for heparin-binding growth factors, cytokines, chemokines and morphogens, and act as cytokine-binding domains, which increases the local concentration and protects them against proteolysis.¹⁵ Owing to the great capacity of HSPG for holding water and binding growth factors, it has been reported to participate in many kinds of biological activities and processes.¹⁶

HSPGs in the ECM can maintain endogenous stem cells or serve as a platform for receiving and directing the integration of transplanted stem cells. The development of gene editing tools allows humans to precisely edit target genes by the deletion, insertion, or site-directed mutagenesis of specific DNA segments.¹⁷ However, the transcript of *HSPG2* is more than 13 000 bp, which exceeds the delivery capacity of traditional virus vectors, including lentiviral, adenovirus and adeno-associated virus vectors. Because of the convenient operation and efficient gene editing ability of the CRISPR/Cas9 system, it has been widely used by researchers in the field of genome editing for species including humans, rats, mice, fish, fruit flies, pigs, rice, wheat and bacteria and exhibits great application potential in disease prevention and intervention, animal and crop breeding, animal disease model development, and other fields.^{18,19}

In this study, we designed and fabricated a specific HSPG2-enriched ECM (ECM^{HSPG2}) based on the CRISPR/Cas9 synergistic activation mediator (SAM) system. The endogenous *HSPG2* was activated and overexpressed in mouse embryonic fibroblasts (MEFs). Additionally, the multiple functions of the ECM^{HSPG2} were evaluated, including the loading of the endogenous basic fibroblast growth factor (bFGF), which is a pivotal factor for neural stem cell (NSC) survival and development and also the promotion of NSC proliferation and differentiation into neurons *in vitro*. This ECM engineering strategy gives an example of manipulating cell-derived ECM and holds great promise for stem-cell based therapy and tissue regeneration.

Results

Endogenous *HSPG2* overexpressing MEFs

The strategic overview of our experiment is presented in Fig. 1. *HSPG2*-overexpressing MEFs were constructed to increase the content level of HSPG2 in a cell-derived ECM. In an SAM system, the RNA-guided nuclease-null Cas9 (dCas9) is fused to a transcriptional activator, VP64, which is reengineered as a programmable transcriptional factor that can activate the transcriptional activity of target genes through the binding of single-guide RNAs (sgRNAs) to the promoter regions.²⁰

Herein, we designed three sgRNAs (named sgRNA-2, sgRNA-3 and sgRNA-4) targeting three different loci within the *HSPG2* promoter. Immunofluorescence staining, real-time PCR and western blot results showed that the expression of HSPG2 was significantly increased in MEFs (Fig. 2 and Fig. S1†). Different sgRNA groups showed about 12.71-, 11.48- and 11.08-fold higher levels of transcription activation than the negative sgRNA infection control (NC) (Fig. 2C), separately,

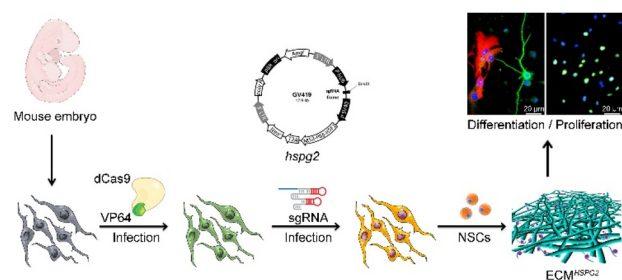


Fig. 1 Illustration of MEF-derived ECM^{HSPG2} fabrication and NSC regulation.

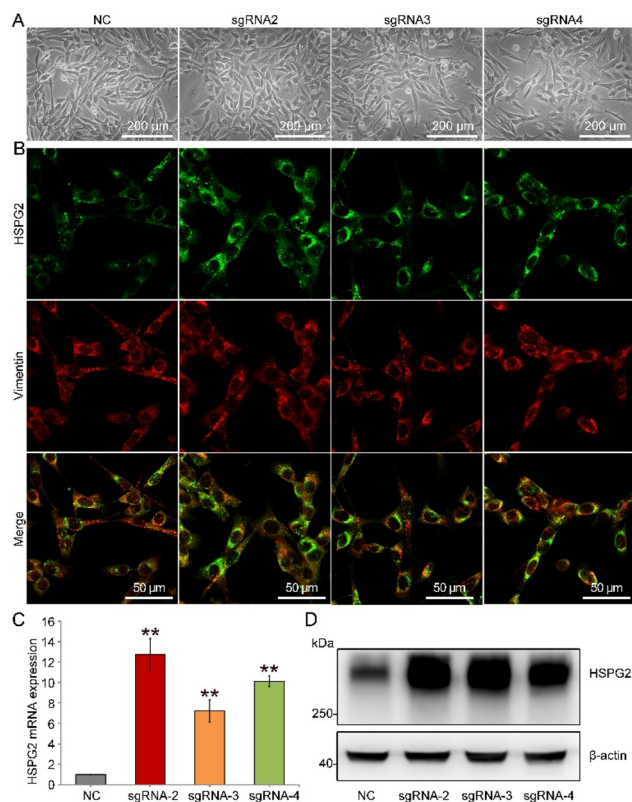


Fig. 2 Endogenous *HSPG2* transcriptional activation in MEFs. (A) Phase-contrast microscopy images of MEFs. (B) Confocal laser scanning images of immunofluorescence staining with anti-*HSPG2* (green) and anti-vimentin (red). (C) Real-time PCR result of *HSPG2* mRNA expression level in MEFs ($n = 3$). (D) Western blot of *HSPG2* protein expression in MEFs. Data are presented as mean \pm SD, $**p < 0.01$ vs. the NC group.

and the sgRNA-2 group was selected in the subsequent experiments, due to its highest expression in both mRNA and protein levels (Fig. 2D). These results indicated that endogenous transcriptional activation of *HSPG2* in MEFs had been achieved through the SAM system.

Fabrication and characterization of cell-derived ECM

The NC or *HSPG2* transcriptional activated MEFs fabricated cell-derived ECMs, named ECM^{NC} or ECM^{HSPG2} , respectively,



as described in Fig. 3A. Upon stimulation with L-ascorbic acid and sodium ascorbate, the cells were embedded in the deposited ECM secreted by themselves and interwoven together. After decellularization, the remaining ECM^{NC} or ECM^{HSPG2} consisting of a large number of interconnected micro- or nano-scale filaments was able to form a highly porous network, as shown by scanning electron microscopy (Fig. 3B). Then, the composition of the cell-derived ECM was identified by immunofluorescence staining and western blot analysis. It was shown that HSPG2 protein content in the ECM^{HSPG2} was significantly higher than that in the ECM^{NC} from both immunofluorescence (Fig. 3C) and western blot results (Fig. 3D). Fibronectin, another important ECM structural protein, was also heavily deposited in the ECM^{HSPG2} compared to in ECM^{NC} without changing its mRNA level. Meanwhile, there was no sig-

nificant difference in the level of vimentin between these two kinds of cell-derived ECMs (Fig. 3D and Fig. S2, S3, S4†).

bFGF is a heparin-binding growth factor which possesses mitogenic and cell-survival promoting functions involved in a variety of biological processes.²¹ It has been proved that bFGF is a crucial factor for NSC proliferation and differentiation.²² According to the results of ELISA, ECM^{HSPG2} could significantly enrich the endogenous bFGF to a level of 232.68 ± 18.56 pg mg⁻¹ of total ECM protein, while the enrichment level of endogenous bFGF was 55.26 ± 12.43 pg mg⁻¹ in the ECM^{NC} group (Fig. 3E). We also detected the other two HSPG2-overexpressing MEFs constructed by sgRNA-3 and sgRNA-4, and they all could enrich the endogenous bFGF, significantly, without obvious changes to the *Fgf2* mRNA (Fig. S2†). Moreover, the amount of bFGF released from ECM^{HSPG2} was significantly more than that from ECM^{NC} at all the time points detected (Fig. 3F). These results showed that MEF-derived ECM^{HSPG2} could not only enrich endogenous bFGF, but also promote the release of bFGF to the surrounding microenvironment, providing it with promising application potential for regulating the NSC cell fate.

NSC proliferation capacity on the cell-derived ECM

The NSCs were initially cultured under serum-free conditions in the presence of bFGF to promote the proliferation of primary neurospheres (Fig. S5A†). The neurospheres were characterized by immunofluorescence staining with protein markers for NSCs including nestin and Sox2 (Fig. S5B†). As investigated by immunofluorescence staining with an anti-nestin antibody, ECM^{NC} and ECM^{HSPG2} both effectively maintained the stemness properties after NSC adherent culture for 7 d (Fig. 4).

The proliferation capacity of NSCs cultured on ECM^{NC} or ECM^{HSPG2} was examined by measuring the ratio of EdU-positive cells after NSCs were maintained in the proliferation medium for 7 d. The EdU/DAPI immunofluorescence results showed that ECM^{HSPG2} promoted NSC proliferation to a significantly higher level than ECM^{NC} (Fig. 5A). The percentage of

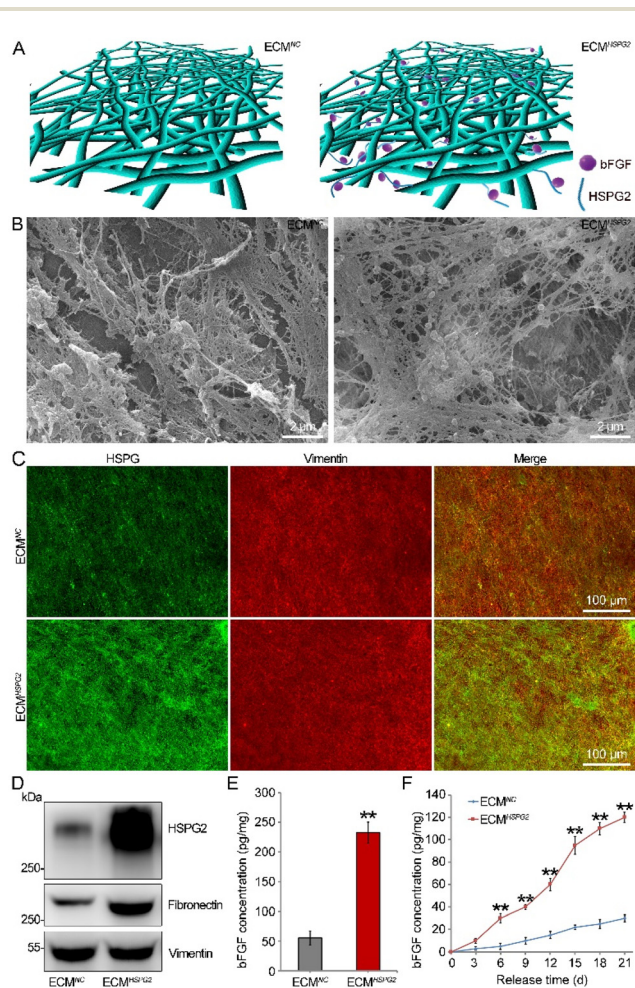


Fig. 3 Morphologies and composition analysis of ECM^{NC} and ECM^{HSPG2}. (A) Schematic diagram of ECM^{NC} and ECM^{HSPG2}. (B) Scanning electron microscopy images of ECM^{NC} and ECM^{HSPG2} (10 000 ×). (C) Immunofluorescence staining images of HSPG2 and vimentin expression in ECM^{NC} and ECM^{HSPG2}. (D) Western blot of HSPG2, fibronectin and vimentin expression in ECM^{NC} and ECM^{HSPG2}. (E) bFGF concentration encapsulated in ECM^{NC} and ECM^{HSPG2} ($n = 3$). (F) bFGF released in ECM^{NC} and ECM^{HSPG2} ($n = 3$). Data are presented as mean \pm SD, ** $p < 0.01$ vs. the ECM^{NC} group.

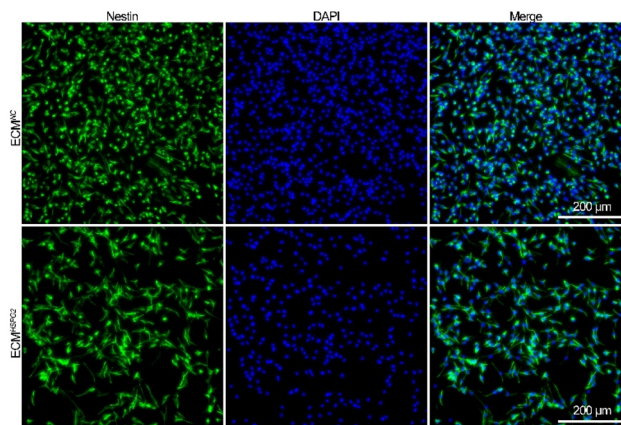


Fig. 4 Immunofluorescence staining against nestin images of NSCs cultured on ECM^{NC} or ECM^{HSPG2} for 7 d.



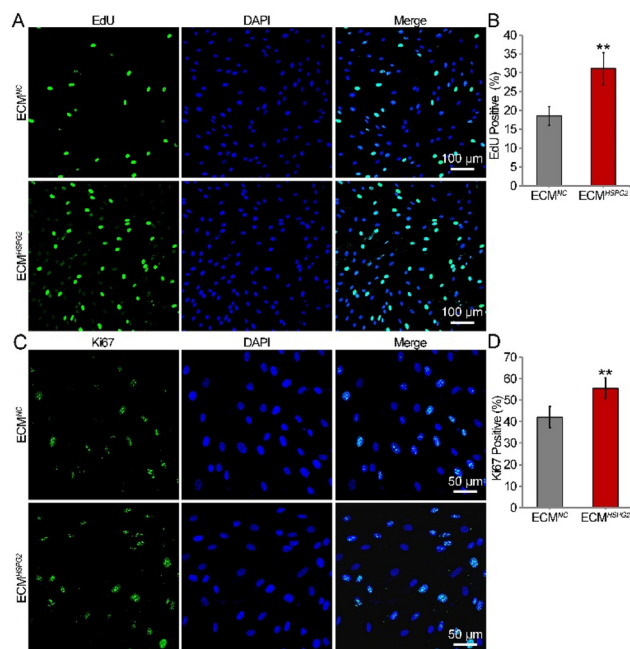


Fig. 5 Proliferation capacities of NSCs cultured on ECM^{NC} or ECM^{HSPG2} for 7 d. (A) EdU immunofluorescence staining of NSCs grown on ECM^{NC} or ECM^{HSPG2}. (B) Percentages of EdU-positive cells ($n = 10$). (C) Ki67 immunofluorescence staining of NSCs grown on ECM^{NC} or ECM^{HSPG2} for 7 d. (D) Percentages of Ki67-positive cells ($n = 10$). Data are presented as mean \pm SD, ** $p < 0.01$ vs. the ECM^{NC} group.

EdU-positive cells in the ECM^{HSPG2} group was significantly higher than that of the ECM^{NC} group ($31 \pm 4\%$ vs. $18 \pm 2\%$, Fig. 5B). The NSC proliferation capacity was also verified by measuring the ratio of Ki67-positive cells (Fig. 5C), and similar to the EdU incorporation result, the percentage of Ki67-positive cells in the ECM^{HSPG2} group was significantly higher than that of the ECM^{NC} group ($55 \pm 4\%$ vs. $42 \pm 5\%$, Fig. 5D). These results indicated that ECM^{HSPG2} could promote the proliferation of NSCs, probably through the enrichment and release of bFGF.

NSC differentiation capacity on cell-derived ECM

In the presence of EGF and bFGF, NSCs remain in a relatively undifferentiated state. With the addition of serum, B27 or N2 supplement and the removal of cytokines to the culture media, NSCs may be induced to differentiate into neurons, astrocytes, and oligodendrocytes.²³ In order to stimulate the proliferation of NSCs before differentiation, bFGF can be added to the medium at the early stage of the differentiation process. However, an alternative differentiation method, which leverages the stimulation of bFGF, could induce increased numbers of neurons. Since ECM^{HSPG2} could significantly enrich and release bFGF (Fig. 3E and F), we next investigated the influence of it on the differentiation of NSCs through culturing NSCs on ECM^{NC} or ECM^{HSPG2} without cytokines. After 14 d of differentiation, immunofluorescence staining showed a vast increase in the number of cells positive for microtubule-associated protein 2 (MAP-2) from $33 \pm 2\%$ on ECM^{NC} to $46 \pm$

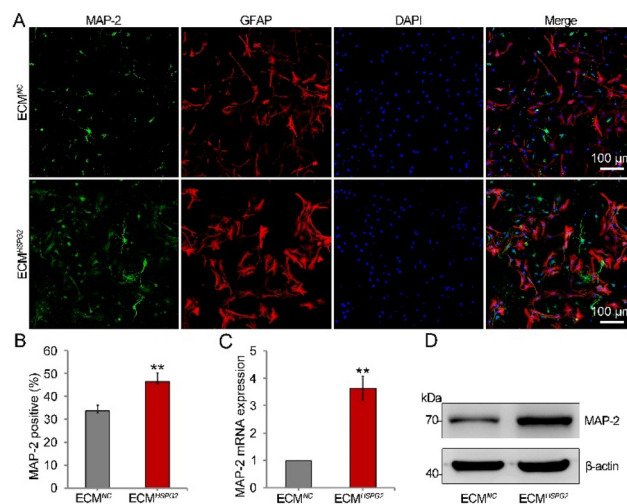


Fig. 6 The differentiation of NSCs into neurons. (A) Representative immunofluorescence images of NSCs were stained with anti-MAP-2 (green) for neurons on ECM^{NC} or ECM^{HSPG2} for 14 d. (B) Percentages of MAP-2-positive cells ($n = 10$). (C) The MAP-2 mRNA expression of NSCs cultured on ECM^{NC} or ECM^{HSPG2} ($n = 3$). (D) The MAP-2 protein expression of NSCs cultured on ECM^{NC} or ECM^{HSPG2}. Data are presented as mean \pm SD, ** $p < 0.01$ vs. the ECM^{NC} group.

3% on ECM^{HSPG2} (Fig. 6A and B). Meanwhile, there was no significant difference between ECM^{NC} and ECM^{HSPG2} groups regarding the number of GFAP-positive cells (Fig. S6A†). For further quantitative analysis, cells were harvested and subjected to real-time PCR and western blot assays. As shown in Fig. 6C and D, compared with the cells on ECM^{NC}, a significant increase in the expression of MAP-2 was achieved in the cells cultured on ECM^{HSPG2}. We also did not observe any significant differences in GFAP mRNA and protein expression between the two conditions (Fig. S6B and C†). These results suggested that ECM^{HSPG2} could increase the differentiation capacity of NSCs, probably through the stimulation of bFGF. Furthermore, owing to its proliferation- and differentiation-promoting properties, this ECM engineering strategy represents a prospective tool for cell therapy and even tissue repair in the future.

Discussion

ECM-mimicking substrates and matrices improve cell culture conditions and focus on tissue engineering applications, establishing superior substrates to remodel and repair diseased tissues and organs.²⁴ In order to improve the efficiency of drug delivery and the function of a drug in an environment mimicking the *in situ* cellular niche, more materials are being developed to simulate the ECM.²⁵ To this end, electrostatic spinning, hydrogels and three-dimensional bio-printing technologies have been used to produce scaffolds from synthetic materials or a limited set of natural polymer blends, but none of these have adequately mimicked the complex morphology and composition of natural ECM.^{26,27} Meanwhile, the



application of tissue-derived ECM scaffolds also has limitations, such as limited donors, potential pathogen transmission and uncontrollable degradation. Therefore, cell-derived ECM has become a promising biomaterial for tissue engineering and regenerative medicine, mainly due to its ability to establish a bionic microenvironment that provides biochemical and physical cues for cells.^{28,29} Purified individual ECM components, including fibrin, laminin, fibronectin, collagen and hyaluronan *etc.*, have no significant effects on cell proliferation and differentiation. In previous work, it has been shown that cell-derived ECM presented a more suitable hydrophilicity than laminin, which is favourable for cell adhesion.⁹ The appropriate hydrophilicity surfaces could adsorb more proteins and transmit signals to the cells through cell adhesion receptors and thereby affect cell survival, growth and differentiation. Various mesenchymal cells or fibroblasts produce cell-derived ECM when stimulated by L-ascorbic acid and 15% fetal bovine serum (FBS), which provide adequate nutrition for the cells. However, the field is progressing towards the expansion/differentiation of NSCs under chemically defined and xeno-free conditions. The composition of FBS is uncertain, nor it is clear whether the composition of FBS could affect the composition of cell-derived ECM deposition. Therefore, the use of serum-free components, such as N2 and B27, to stimulate cell-derived ECM formation, or the use of different batches or even different brands of FBS tests, should be further validated in the future.

In addition, cell-derived ECM with specific functions can be designed and fabricated by altering the expression of specific ECM protein components in the originating cells. The cell-derived ECM enriched with a collagen-binding domain fused with membrane metalloendopeptidase or an insulin-degrading enzyme could reduce the aggregation of A β peptides. This prevents the formation of amyloid plaques and also suppresses the phosphorylation of Tau protein, providing a cell-derived ECM that can be potentially used in the treatment of Alzheimer's disease.³⁰ Farhang N *et al.*³¹ demonstrated the increased expression and deposition of aggrecan and collagen II without exogenous growth factors in ECM pellet culture. Fibronectin knockout by CRISPR/Cas9 in human infrapatellar fat pad-derived stem cells (IPFSCs) and the derived decellularized ECM could inhibit the proliferation of high-passage IPFSCs along with a decline in CDH2 expression.³²

The SAM system enables the robust transcriptional activation of endogenous genes targeted by sgRNAs that bind within 200 bp upstream of the transcription start site.³³ This system fuses RNA-guided dCas9 with a well-characterized transcription regulatory domain, using predesigned sgRNAs to direct the binding of the transcriptional complex to the target sites. Using nuclease-null dCas9 protein, the complex can be targeted to specific sites without cutting or altering the genomic DNA. After dCas9 binds the targeted DNA sequence, the fused transcription regulatory domains recruit inhibitory or activating effectors to modify gene expression.³⁴ Therefore, we could apply the SAM system to precisely design and develop cell-derived ECM with encapsulated growth factors.

Indeed, various stem cell types adapt to different specific ECM proteins, and some ECM proteins have specialized functions that are restricted to distinct stem cell niches, for stem cell survival and self-renewal *in vivo* and *in vitro*. For example, tenascin C and osteopontin are specifically present in hematopoietic stem cell niches, whereas β -1 integrins are predominantly expressed in epidermal stem cell niches.³⁵ Fibronectin induces the differentiation of either myoblasts into skeletal muscle cells or adipose tissue-derived stem cells into endothelial cells.^{36,37} Proteoglycans can be considered as one of the first critical ECM components for maintaining normal cell function and tissue development.³⁸ With multiple biological functions in development and disease, HSPG2 is a key proteoglycan.³⁹ Importantly, HSPG2 regulates cellular behaviour and biological processes by binding cytokines, growth factors and chemokines, such as bFGF.^{15,40}

Like other cytokines, bFGF is unstable under physiological conditions and is likely to be broken down by proteolytic degradation when in an unbound state. When injected *in vivo*, the biological functions of bFGF were reduced due to diffusion, enzymolysis, and weak binding with co-receptors. However, HSPG2 protects bFGF from proteolytic degradation, thanks to its physical structure, and it can also induce bFGF biological activities by acting as a co-receptor.¹⁶ In addition to bFGF, other cytokines that possess binding affinity to HSPG2, such as VEGF, BMP-9, EGF, FGF8 and SHH, are also considered to be pivotal for stem cell fate and function.^{14,16,41,42} Our designed ECM^{HSPG2} is an ideal delivery carrier that enriches the endogenous and exogenous bFGF, which can be further distributed at the injury site and degraded by proteolysis under normal physiological conditions. In this study, with enriched bFGF, ECM^{HSPG2} promotes NSC proliferation and their differentiation into the neurons, which signifies that ECM^{HSPG2} has the potential to become an agent for stem cell transplantation.

As a major component of ECM in the basement membrane, HSPG also binds with many other ECM proteins to form the skeleton of the ECM, making HSPG a link molecule targeting ECM proteins. Herein, we showed that HSPG2 is capable of facilitating ECM remodeling and the deposition of structural matrix proteins, such as fibronectin, which plays an essential role in cell adhesion, migration and the development of embryonic vascular structures.⁴³ Thus, we suggest that using this ECM engineering strategy will benefit not only fundamental research about the ECM function, but also clinical applications of ECM in cell therapy and tissue repair.

Experimental

All animal procedures were performed in accordance with the Guidelines for the Care and Use of Laboratory Animals of Suzhou Institute of Nano-Tech and Nano-Bionics, Chinese Academy of Sciences, and approved by the Animal Ethics Committee of Suzhou Institute of Nano-Tech and Nano-Bionics, Chinese Academy of Sciences. Efforts were made to



minimize the number of animals used and any discomfort experienced. Detailed information on essential materials used in this study can be found in the ESI.†

Isolation and culture of MEFs

Skin from an E12.5 fetal C57BL/6 mouse was collected in a bacteria-free environment and then cut into small pieces and spread onto a culture dish. The pieces were continuously cultured for 4–7 d in high-glucose DMEM supplemented with 10% fetal bovine serum (FBS). The MEFs were purified using the trypsin digestion-adherence method.

Construction of endogenous HSPG2 transcriptionally activated MEFs

CRISPR plasmids and lentiviral vectors for dCAS9-VP64-Puro and gRNA LV-sgRNA-MS2-P65-HSF1-Neo (GV419) were constructed by Genechem (Shanghai, China). MEFs infected with dCAS9-VP64-Puro and negative gRNA were used as the negative control. The sequences of sgRNAs used in this article are listed in Table S1.† MEFs were seeded in 6-well plates at a density of 1×10^4 cells per cm^2 and transduced at 10 MOI with dCAS9-VP64-Puro. Cells were subcultured and selected with $2 \mu\text{g mL}^{-1}$ puromycin. After two weeks of selection culture, cells were seeded in 6-well plates at a density of 1×10^4 cells per cm^2 and infected with 10 MOI Lenti-MS2-p65-HSF1. Cells were subcultured and selected with $10 \mu\text{g mL}^{-1}$ G418. After stable cell lines were obtained, the HSPG2 expression level was assessed by real-time PCR, western blot assay and immunofluorescence staining.

Production of cell-derived ECM^{NC} and ECM^{HSPG2}

Cell-derived ECMs were fabricated by stimulating the MEFs or HSPG2 transcriptionally activated MEFs, according to our previously published work.⁹ In brief, the culture substrates were pre-treated by incubating with 0.5% gelatin at 37 °C overnight and exposed to ultraviolet rays for 2 h to enhance crosslinking. Cells were seeded on the substrates at the same density of 5×10^4 cells per cm^2 . After the cells were cultured to 100% confluence, the medium was changed to DMEM with 15% FBS and 50 mg mL^{-1} L-ascorbic acid and 100 mg mL^{-1} sodium ascorbate for 10 d. After the stimulation of ECM formation, the cells were washed with deionized water for 20 min, followed by treatments with 0.5% Triton X-100 plus 1% deoxycholate for 10 min and with 100 U mL^{-1} DNase I for 30 min at 37 °C.

Characterization of the binding and release of bFGF

The bFGF binding and release assay was performed using an FGF2 (bFGF) Mouse ELISA Kit according to the manufacturer's instructions. Freshly prepared cell-derived ECMs were dissociated in RIPA lysis buffer with a protease inhibitor, and the supernatant was obtained by centrifugation at 12 000g. The concentration of ECM-bound bFGF was normalized to the total ECM protein content, detected using a BCA kit. To measure the amount of bFGF contained in ECM, cell-derived ECMs were placed at 37 °C for 0, 3, 6, 9, 12, 15, 18, and 21 d,

and the supernatant was collected and tested using the ELISA kit as described above.

Isolation and culture of NSCs

The cerebral cortex was dissected from the brain of fetal mice at E14 and then digested with trypsin at 37 °C for 2 min. After gentle dissociation into small pieces using a pipette, single cells were acquired by centrifugation. The cells were re-suspended and cultured in a proliferation medium containing NeuroCult Basal Medium with 10% NeuroCult Proliferation Supplement, 1% PS, 20 ng mL^{-1} of human recombinant epidermal growth factor (EGF), and 10 ng mL^{-1} of human recombinant bFGF. The cells were expanded as spheres, and the medium was half-refreshed every 3 d. In this study, passage 3 and 5 NSCs were used for further experiments.

Proliferation and differentiation of NSCs

The NSCs were cultured in the proliferation medium as previously mentioned. For the differentiation study, the NSC spheres were digested into single cells with Accutase and seeded on the ECM at a density of 2×10^5 cells per cm^2 in the proliferation medium for 12 h, and then the medium was changed to the differentiation medium containing NeuroCult Basal Medium with 2% B27, 2 μM glutamine, and 1% PS for 14 d. The differentiation medium was replaced every 3 d.

Immunofluorescence staining

MEFs, ECM and NSCs were fixed in 4% paraformaldehyde at room temperature for 20 min, washed with PBS and blocked with 5% normal goat serum containing 0.1% Triton X-100 at room temperature for 1 h. Subsequently, the cells were incubated with primary antibodies specific to HSPG2 (1 : 200), vimentin (1 : 200), Nestin (1 : 200), Sox-2 (1 : 200), Ki67 (1 : 200) and MAP-2 (1 : 200) at 4 °C overnight. After washing, the cells were incubated with Alexa Fluor 488 or 594 labelled secondary antibodies in the dark at room temperature for 2 h. The cell nuclei were counterstained with 5 $\mu\text{g mL}^{-1}$ DAPI. Fluorescence microscopy images were collected using a confocal laser scanning microscope with the same magnification and the same fluorescence intensity (Olympus, Japan). The percentages of EdU-, Ki67- and MAP2-positive cells were calculated from ten random fields, and each experiment was performed in triplicate.

Real-time PCR

Total RNA was isolated from MEFs and NSCs with TRIzol reagent, and the concentration was quantified using a Nano100 spectrophotometer (Thermo, USA). First-strand cDNA was synthesized from 1 μg total RNA (A260/280: 1.8–2.0, A260/230: 2.0–2.2) using a first-strand cDNA synthesis kit. Thereafter, real-time PCR was carried out using the obtained cDNA with SYBR Mixture for 40 cycles. The $2^{-\Delta\Delta C_t}$ method was used to calculate the target gene relative mRNA expression. The primers were synthesized by Genewiz (Suzhou, China), and the sequences are listed in Table S1.† GAPDH was used as



an endogenous control, and each experiment was performed in triplicate.

Western blot

MEFs, ECM and NSCs were lysed in an ice-cold RIPA buffer with a protease inhibitor. The lysates were then centrifuged at 12 000g for 20 min to collect the supernatant. The protein concentration was determined with a BCA assay kit and denatured in boiling water for 5 min. Equal amounts of proteins were separated by SDS-PAGE and transferred to the PVDF membrane. After being blocked for 1 h at room temperature, the membrane was then incubated with primary antibodies specific to HSPG2 (1:1000), fibronectin (1:1000), vimentin (1:1000), MAP-2 (1:1000) and β -actin (1:1000) at 4 °C overnight. The membranes were washed with TBST three times and then incubated with HRP-conjugated secondary antibodies (1:1000) at room temperature for 2 h. The protein bands were visualized using an ECL substrate under an LAS4000 imaging system (Fuji Film, Japan). β -Actin was used as an endogenous control, and each experiment was performed in triplicate.

Scanning electron microscopy imaging

Fresh prepared ECM samples were washed three times with PBS and fixed with 4% paraformaldehyde for 20 min at room temperature, followed by post-fixation in 2.5% glutaraldehyde for 30 min at 4 °C. The samples were dehydrated in 50%, 70%, 80%, 90%, and 100% ethanol for 10 min, respectively. After being replaced with 100% *tert*-butanol, they were frozen at -20 °C for 30 min and lyophilized in a vacuum dryer. The ECM samples were coated with a gold film before observation under a scanning electron microscope (Quanta 400 FEG, FEI, USA).

Statistical analysis

All experiments were performed in triplicate, and the data are shown as the means \pm SD of three separate experiments. Statistical analysis was performed using one-way analysis of variance followed by Dunnett's two-tailed test, and then Student's independent samples *t*-test was performed to compare the difference between the two groups. Probability values of $**p < 0.01$ were considered significant.

Conclusions

Although various artificial materials have been exploited to mimic the ECM regulation of stem cell function, there were almost no reports on how to make natural cell-derived ECM that is more appropriate for stem cell study and application. In this study, we fabricated a specific functional cell-derived ECM based on the SAM system. In addition, the ECM protein can also be used to enrich bFGF suggesting that ECM^{HSPG2} is a promising biomaterial candidate for the stem cell niche. ECM^{HSPG2} promoted NSC proliferation and differentiation into neurons *in vitro*. This research will provide a precise design

strategy to develop a functional cell-derived ECM for stem cell-based biomaterials research and regenerative medicine. However, the mechanism by which HSPG2 increases the fibronectin deposition and bFGF binding efficiency requires further study.

Author contributions

Y. L. Y. and Z. Y. X.: conceptualization and writing – original draft; Z. Y. X., and Z. W. L.: data curation; W. Q. W., Z. Z. C., H. F. and H. Y.: investigation; and M. S. C. and C. G. S.: funding acquisition and writing – review & editing.

Conflicts of interest

There are no conflicts to declare.

Acknowledgements

This work was supported by grants from the National Natural Science Foundation of China (31700831) and Guangdong Province Joint Fund (2019B1515120090).

References

- 1 D. T. Scadden, *Nature*, 2006, **441**, 1075.
- 2 D. Lucas, *Adv. Exp. Med. Biol.*, 2017, **1041**, 5.
- 3 G. M. Crane, E. Jeffery and S. J. Morrison, *Nat. Rev. Immunol.*, 2017, **17**, 573.
- 4 M. Votteler, P. J. Kluger, H. Walles and K. Schenke-Layland, *Macromol. Biosci.*, 2010, **10**, 1302.
- 5 Y. Xu, J. Zhou, C. Liu, S. Zhang, F. Gao, W. Guo, X. Sun, C. Zhang, H. Li, Z. Rao, S. Qiu, Q. Zhu, X. Liu, X. Guo, Z. Shao, Y. Bai, X. Zhang and D. Quan, *Biomaterials*, 2021, **268**, 120596.
- 6 S. Yi, F. Ding, L. Gong and X. Gu, *Curr. Stem Cell Res. Ther.*, 2017, **12**, 233.
- 7 Y. Kang, S. Kim, J. Bishop, A. Khademhosseini and Y. Yang, *Biomaterials*, 2012, **33**, 6998.
- 8 E. Chermnykh, E. Kalabusheva and E. Vorotelyak, *Int. J. Mol. Sci.*, 2018, **19**, 1003.
- 9 L. Yang, Z. Jiang, L. Zhou, K. Zhao, X. Ma and G. Cheng, *RSC Adv.*, 2017, **7**, 45587.
- 10 A. D. Theocharis, S. S. Skandalis, C. Gialeli and N. K. Karamanos, *Adv. Drug Delivery Rev.*, 2016, **97**, 4.
- 11 J. Halper and M. Kjaer, *Adv. Exp. Med. Biol.*, 2014, **802**, 31.
- 12 L. M. Jenkins, B. Horst, C. L. Lancaster and K. Myhre, *Cytokine Growth Factor Rev.*, 2018, **39**, 124.
- 13 N. K. Karamanos, Z. Piperigkou, A. D. Theocharis, H. Watanabe, M. Franchi, S. Baud, S. Brézillon, M. Götte, A. Passi, D. Vigetti, S. Ricard-Blum, R. D. Sanderson, T. Neill and R. V. Iozzo, *Chem. Rev.*, 2018, **118**, 9152.
- 14 M. Xie and J. P. Li, *Cell. Signalling*, 2019, **54**, 115.



- 15 S. Sarrazin, W. C. Lamanna and J. D. Esko, *Cold Spring Harbor Perspect. Biol.*, 2011, **3**(7), a004952.
- 16 J. Shi, C. Fan, Y. Zhuang, J. Sun, X. Hou, B. Chen, Z. Xiao, Y. Chen, Z. Zhan, Y. Zhao and J. Dai, *Biomater. Sci.*, 2019, **7**, 5438.
- 17 F. Akram, U. H. Ikram, Z. Ahmed, H. Khan and M. S. Ali, *Protein Pept. Lett.*, 2020, **27**, 931.
- 18 C. Lyu, J. Shen, R. Wang, H. Gu, J. Zhang, F. Xue, X. Liu, W. Liu, R. Fu, L. Zhang, H. Li, X. Zhang, T. Cheng, R. Yang and L. Zhang, *Stem Cell Res. Ther.*, 2018, **9**, 92.
- 19 C. Jiang, L. Meng, B. Yang and X. Luo, *Clin. Genet.*, 2020, **97**, 73.
- 20 L. A. Gilbert, M. H. Larson, L. Morsut, Z. Liu, G. A. Brar, S. E. Torres, N. Stern-Ginossar, O. Brandman, E. H. Whitehead, J. A. Doudna, W. A. Lim, J. S. Weissman and L. S. Qi, *Cell*, 2013, **154**, 442.
- 21 D. Nawrocka, M. A. Krzyscik, L. Opalinski, M. Zakrzewska and J. Otlewski, *Int. J. Mol. Sci.*, 2020, **21**, 4108.
- 22 C. Li, L. H. Che, L. Shi and J. L. Yu, *J. Cell. Biochem.*, 2017, **118**, 3875.
- 23 N. Li, Qi. Zhang, S. Gao, R. Huang, L. Wang, L. Liu, J. Dai, M. Tang and G. Cheng, *Sci. Rep.*, 2013, **3**, 1604.
- 24 H. Lu, T. Hoshihara, N. Kawazoe, I. Koda, M. Song and G. Chen, *Biomaterials*, 2011, **32**, 9658.
- 25 J. Hwang, M. O. Sullivan and K. L. Kiick, *Front. Bioeng. Biotechnol.*, 2020, **8**, 69.
- 26 M. Keshvaridoostchokami, S. S. Majidi and P. Huo, *Nanomaterials*, 2020, **11**, 21.
- 27 J. Wang, Y. Yu, J. Guo, W. Lu, Q. Wei and Y. Zhao, *Adv. Biosyst.*, 2020, **4**(2), e1900238.
- 28 Y. Yang, H. Lin, H. Shen, B. Wang, G. Lei and R. S. Tuan, *Acta Biomater.*, 2018, **69**, 71–82.
- 29 J. C. Silva, M. S. Carvalho, K. Xia, J. M. S. Cabral, C. L. da Silva, F. C. Ferreira, D. Vashishth and R. J. Linhardt, *Methods Cell Biol.*, 2020, **156**, 85.
- 30 S. Zhang, T. Xiao, Y. Yu, Y. Qiao, Z. Xu, J. Geng, Y. Liang, Y. Mei, Q. Dong, B. Wang, J. Wei and G. Suo, *J. Tissue Eng. Regener. Med.*, 2019, **13**, 1759.
- 31 N. Farhang, B. Davis, J. Weston, M. Ginley-Hidinger, J. Gertz and R. D. Bowles, *Tissue Eng., Part A*, 2020, **26**, 1169.
- 32 Y. Wang, Y. Fu, Z. Yan, X. B. Zhang and M. Pei, *Front. Bioeng. Biotechnol.*, 2019, **7**, 321.
- 33 S. Konermann, M. D. Brigham, A. E. Trevino, J. Joung, O. O. Abudayyeh, C. Barcena, P. D. Hsu, N. Habib, J. S. Gootenberg, H. Nishimasu, O. Nureki and F. Zhang, *Nature*, 2015, **517**, 583.
- 34 P. Mali, J. Aach, J. H. Lee, D. Levner, L. Nip and G. M. Church, *Nat. Methods*, 2013, **10**, 403.
- 35 S. Stier, Y. Ko, R. Forkert, C. Lutz, T. Neuhaus, E. Grünwald, T. Cheng, D. Dombkowski, L. M. Calvi, S. R. Rittling and D. T. Scadden, *J. Exp. Med.*, 2005, **201**, 1781.
- 36 S. Heydarkhan-Hagvall, K. Schenke-Layland, J. Q. Yang, S. Heydarkhan, Y. Xu, P. A. Zuk, W. R. MacLellan and R. E. Beygui, *Cells Tissues Organs*, 2008, **187**, 263–274.
- 37 M. A. Lan, C. A. Gersbach, K. E. Michael, B. G. Keselowsky and A. J. Garcia, Myoblast proliferation and differentiation on fibronectin-coated self assembled monolayers presenting different surface chemistries, *Biomaterials*, 2005, **26**, 4523–4531.
- 38 N. Hassan, B. Greve, N. A. Espinoza-Sanchez and M. Gotte, *Cell. Signalling*, 2021, **77**, 109822.
- 39 H. Kaneko, M. Ishijima, I. Futami, N. Tomikawa-Ichikawa, K. Kosaki, R. Sadatsuki, Y. Yamada, H. Kurosawa, K. Kaneko and E. Arikawa-Hirasawa, *Matrix Biol.*, 2013, **32**, 178.
- 40 J. R. Bishop, M. Schuksz and J. D. Esko, *Nature*, 2007, **446**, 1030.
- 41 D. C. Kraushaar, S. Rai, E. Condac, A. Nairn, S. Zhang, Y. Yamaguchi, K. Moremen, S. Dalton and L. Wang, *J. Biol. Chem.*, 2012, **287**, 22691.
- 42 A. Wade, A. McKinney and J. J. Phillips, *Biochim. Biophys. Acta*, 2014, **1840**, 2520.
- 43 M. Marchand, C. Monnot, L. Muller and S. Germain, *Semin. Cell Dev. Biol.*, 2019, **89**, 147.

